Journal of Colloid and Interface Science 563 (2020) 27–32

Contents lists available at ScienceDirect

Journal of Colloid and Interface Science

journal homepage: www.elsevier.com/locate/jcis

KOH-doped polybenzimidazole membrane for direct hydrazine fuel cell

Yucheng Wang [a], Qi Wang [a], Li-yang Wan [a], Yu Han [a], Yuhao Hong [a], Long Huang [c], Xiaodong Yang [d], Yuesheng Wang [b], Karim Zaghib [b], Zhiyou Zhou [a]

[a] State Key Laboratory of Physical Chemistry of Solid Surfaces, Collaborative Innovation Center of Chemistry for Energy Materials, College of Chemistry and Chemical Engineering, Xiamen University, Xiamen 361005, China
[b] Center of Excellence in Transportation Electrification and Energy Storage, Hydro Québec, Québec J3 × 1S1, Canada
[c] Kunming Institute of Precious Metals, Kunming 650106, China
[d] College of Materials Science & Engineering, Huaqiao University, Xiamen 361021, China

HIGHLIGHTS

- A KOH-doped PBI membrane was applied in DHFC for the first time.
- The influence of anolyte, membrane thickness and oxygen humidity was investigated.
- A peak power density of 0.708 W cm^{-2} was achieved.

GRAPHICAL ABSTRACT

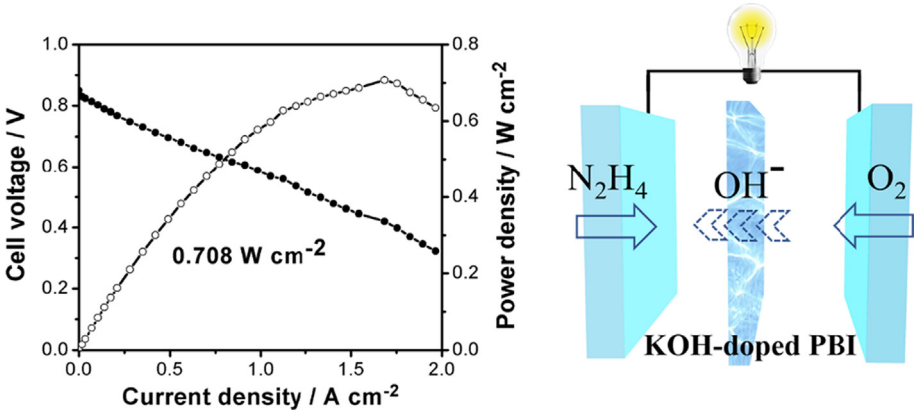

ARTICLE INFO

Article history:
Received 9 October 2019
Accepted 12 December 2019
Available online 13 December 2019

Keywords:
Direct hydrazine fuel cell
Electrolyte membrane
KOH-doping
Polybenzimidazole (PBI)
Power density

ABSTRACT

Alkaline direct hydrazine (N_2H_4) fuel cells (DHFCs) are considered one of the most promising liquid-fed fuel cells because of their high energy density, high theoretical voltage, and zero carbon dioxide (CO_2) emissions. However, the lack of a suitable electrolyte membrane impedes the further development of alkaline DHFC. Herein, a potassium hydroxide (KOH)-doped polybenzimidazole (PBI) membrane is applied in alkaline DHFCs, and the detailed operating conditions are investigated for the first time. With optimal KOH and N_2H_4 concentrations in the anolyte, membrane thickness, and cathode gas humidity, the DHFC gives a peak power density of 0.708 W cm^{-2}. The results of this study demonstrate the promising application of PBI membranes in DHFC and provide a platform to evaluate the performance of catalysts synthesized for DHFC.

1. Introduction

Direct hydrazine fuel cells (DHFCs) have been considered as one of the most promising low-temperature fuel cells because of the following advantages: (1) accessible fuel supply; (2) convenient storage and transport; (3) high energy density of hydrazine; (4) high theoretical open circuit voltage of 1.56 V with oxygen as the oxidant; and (5) zero CO_2 emissions [1]. Currently, three typical configurations for DHFC exist. The first configuration is proton exchange membrane (PEM)-based fuel cells that uses Nafion as the proton exchange membrane [2]. However, it is suggested that

E-mail addresses: Wang.Yuesheng@hydro.qc.ca (Y. Wang), Zaghib.Karim@hydro.qc.ca (K. Zaghib), zhouzy@xmu.edu.cn (Z. Zhou)

https://doi.org/10.1016/j.jcis.2019.12.046
0021-9797/

the crossover of $N_2H_5^+$ ions from anode to cathode through the Nafion membrane and the resulting mixed potential severely limit the polarization performance of PEM-based DHFC [3]. To suppress the crossover of $N_2H_5^+$ ions and meanwhile avoid sluggish oxygen reduction reactions, some researchers have proposed a second bipolar-configuration DHFC using H_2O_2 as the oxidant, in which the N_2H_4 is oxidized in alkaline media on one side of the membrane, while H_2O_2 is reduced in acidic media on the other side of the membrane [4]. Nevertheless, some problems still existed in this configuration, such as the oxidative attack of H_2O_2 toward the Nafion membrane and catalysts as well as the decomposition of H_2O_2 at operation temperature (60–80 °C) [5,6]. Moreover, the abrupt acid-alkaline interface is not easy to maintain, which imposes a challenge on the long-term durability of DHFCs. The third configuration for DHFC with mild operation conditions is alkaline fuel cell with oxygen or air as the oxidant [7,8]. Under alkaline conditions, the crossover of $N_2H_5^+$ ions is significantly suppressed [8] and the kinetics of the oxygen reduction reaction (ORR) is very fast; consequently, non-precious metal catalysts can be used to lower the cost of the DHFC [9]. Notably, the performance of this configuration is highly dependent on the property of the electrolyte membrane. Currently, the most commonly used electrolyte membrane for DHFC is ammonium-type anion exchange membrane [10–13]. Using the ammonium-type anion exchange membrane, the highest peak power density of DHFC obtained with oxygen as oxidant was 0.617 W cm^{-2} [11]. Considering the high theoretical energy density and open circuit voltage (1.65 V with oxygen as oxidant) of DHFC [1], there is still room for the improvement of the performance of DHFC. Therefore, it is desirable to identify a suitable electrolyte membrane to further improve the polarization performance of alkaline DHFC.

Polybenzimidazole (PBI) membranes are widely used in high-temperature proton exchange membrane fuel cells (HT-PEMFCs) after H_3PO_4 doping [14–16]. In addition to HT-PEMFCs, KOH-doped PBI membranes also exhibit high OH^- conductivity and have been applied in alkaline hydrogen/oxygen polymer electrolyte membrane fuel cells and direct alcohol fuel cells, providing high power density [17–20]. From this point, KOH-doped PBI membrane is also expected to perform well in alkaline DHFC. So far, the application of KOH-doped PBI membranes in DHFC has not been reported yet.

In our recent study, the efficiency of KOH-doped PBI membrane in alkaline DHFC was initially demonstrated [21], but more detailed operating conditions were still lacking. In this study, a KOH-doped PBI membrane was applied in alkaline DHFC, and the influence of KOH and N_2H_4 concentrations in the anolyte, membrane thickness, and cathode gas humidity on cell performance was investigated. A solution containing 1.5 M N_2H_4 and 6 M KOH was used as the anolyte, a 20-μm thick membrane was adopted as the electrolyte membrane, and 100% RH humidified oxygen was used as oxidant. A peak power density of 0.708 W cm^{-2} was achieved at 80 °C. Compared with two other commonly used membranes [Na^+-type Nafion membrane, ammonium-type anion ion exchange membrane], the KOH-doped PBI membrane exhibited excellent membrane permeation properties and the highest ion conductivity, consequently obtaining the highest peak power density.

2. Materials and methods

2.1. Chemicals and materials

All chemicals were purchased and used without further purification. KOH (99%), NaOH (99%) and isopropanol (>99%) were purchased from Sinopharm Chemical Reagent Co., Ltd (China). PTFE slurry (15 wt%), nickel foam, gas diffusion layer with microporous layer were purchased from Sunlaite Technology Co., Ltd (China). Pt/C electrocatalyst (20 wt%) for hydrazine oxidation and ORR were purchased from Johnson Matthey. Nafion solution (5 wt%) and Nafion membrane (N211) were purchased from DuPont Corp. PBI membranes [poly(2,2-(m-phenylene)-5,5-bibenzimidazole)] were supplied by Shengjun Plastic Technology Co., Ltd. Ammonium-type anion exchange membrane, QAPS, was supplied by Wuhan university [22]. De-ionized water with a specific resistance of 18.2 MΩ·cm (Milli-Q) was used to prepare the solutions.

2.2. Membrane electrode assembly (MEA) preparation

The membrane electrode assembly (MEA) was prepared through the hot-pressing method. The anode was fabricated by the following procedure. Six milligrams of commercial Pt/C catalyst (20 wt%) and 200 μL PTFE slurry (15 wt%) were dispersed in 200 μL isopropanol. The anode Pt loading was 1.0 mg cm^{-2}. The obtained slurry was coated on a nickel foam (1.14 cm^2) and then immersed in a 6.0 M KOH solution for 12 h. The cathode was fabricated by a similar method: 20 mg commercial Pt/C catalyst (20 wt%, Johnson Matthey) and 200 μL Nafion solution (5 wt%, Dupont) were added to 2 mL isopropanol. The resulting cathode ink was coated on a gas diffusion layer, dried at 80 °C under vacuum, and then, immersed in 6.0 M KOH solution for 24 h. During the soak process, H^+-type Nafion was exchanged into K^+-type to avoid the occurrence of acid-alkaline reaction between H^+-type Nafion and OH^- during the ORR process. The cathode Pt loading was controlled at 0.58 mg cm^{-2}. Here, the PBI membrane/H^+-type Nafion 211 membrane (Dupont)/ammonium-type anion exchange membrane (QAPS, Cl^--type) was pre-treated with 6 M KOH or NaOH solution at 60 °C for 3 h and then at room temperature for 24 h. During the soak process, H^+-type Nafion 211 membrane turned to Na^+-type while Cl^- in the QAPS was exchanged by OH^-. PBI was completely ionized and the excess solvated KOH provided high through-plane conductivity (Fig. S1) [23]. Finally, the MEA was fabricated by hot-pressing the cathode, anode, KOH-doped PBI membrane (or the other two membranes), and the required size of gasket at 80 °C and 1 MPa for 30 s. Need to note that the hot-pressing time and temperature should be precisely controlled to avoid the dry-out and precipitation of KOH-doped PBI membrane. For example, if the hot-pressing temperature is higher, a shorter hot-pressing time should be selected (i.e., 130 °C for 2 s). Cold-pressing may be an efficient method to avoid evaporation of water from the KOH-doped membranes, but it may lead to insufficient contact between electrodes and electrolyte membrane.

2.3. Fuel cell evaluation

Polarization curves were obtained using the Model 850e fuel cell test system (Scribner Associates Inc). Different concentrations of anolyte were fed as fuel at a flow rate of 1.0 mL min^{-1}, while humidified oxygen was fed as the oxidant at a flow rate of 0.1 standard liter per minute (SLPM) at different dew point temperatures (40 °C, 60 °C, 80 °C, and 90 °C). The cell temperature was set to 80 °C. The polarization performance of DHFC was measured at ambient pressure, and the active area of the MEA was 1.14 cm^2. After keeping the MEA under these conditions for 30 min, a constant open circuit voltage (OCV) was obtained, which was followed by the polarization performance test. The polarization data were recorded in the galvanostatic polarization mode, and each point was maintained for 1 min to obtain the steady voltage and cell ohmic resistance (1000 Hz). To validate the rationality of using high-frequency resistance as an indicator of cell ohmic resistance, another method to determine cell ohmic resistance by analyzing

polarization curves was also compared (Fig. S2, taking Fig. 3 as example). To evaluate the permeation property of the membranes, 1.5 M N_2H_4 in 6 M KOH solution and humified N_2 were fed to the anode and cathode, respectively. The crossover current was measured by linear sweep voltammetry (LSV) method at a scan rate of 2 mV s^{-1} from 0 V to 0.8 V. Based on the oxidation currents, the permeability of N_2H_4 for the three membranes was calculated.

3. Results and discussion

3.1. Effects of anolyte composition

3.1.1. KOH concentration

Fig. 1a shows the influence of KOH concentration in the anolyte on the open circuit voltage (OCV) of alkaline DHFC with KOH-doped polybenzimidazole (PBI) as the membrane. When the KOH concentration in the anolyte increased from 2 M to 8 M, the OCV of DHFC increased form 0.85 V to 0.917 V, accordingly. The increased OCV was attributed to the suppression of OH^- in the crossover of $N_2H_5^+$ ions [24]. As the KOH concentration increased from 2 M to 6 M, the peak power density of DHFC increased from 0.196 W cm^{-2} to 0.506 W cm^{-2} and then declined slightly to 0.434 W cm^{-2} when KOH concentration reached 8 M (Fig. 1c and d). Because the addition of KOH could suppress the crossover of $N_2H_5^+$ ions (Fig. 1a) and improve ion conductivity (Fig. 1b), it is expected that the increase of KOH concentration in the anolyte increased the cell polarization performance of DHFC when KOH concentration was below 6 M [25]. However, as KOH concentration increased in the anolyte, the viscosity of the anolyte would also increase and the movability of the charge carrier would decrease, thus deteriorating cell performance [24]. Therefore, the cell polarization performance of DHFC decreased when high concentration of KOH solution (8 M) was used.

3.1.2. N_2H_4 concentration

With optimized KOH concentration (6 M), the influence of N_2H_4 concentration on the cell polarization performance of DHFC was also investigated. Fig. 2a shows the variation of OCV of DHFC with increasing N_2H_4 concentration in the anolyte. When N_2H_4 concentration increased from 0.1 M to 2.5 M, the OCV decreased from 0.944 V to 0.793 V. The decreased OCV can be explained by the mixed potential caused by the crossover of N_2H_4 [11,26]. As high-concentrated N_2H_4 can lead to severe N_2H_4 crossover but can also increase fuel utilization efficiency [11], it is expected that the cell polarization performance would increase first and then decline with increasing N_2H_4 concentration. Fig. 2b-c shows the polarization performance of DHFC fed with different concentrations of N_2H_4 in 6 M KOH solution. As expected, the peak power density of DHFC increased when N_2H_4 concentration increased from 0.1 M to 1.5 M and then declined at 2.0 M. With 1.5 M N_2H_4 in 6 M KOH solution, the peak power density of DHFC reached 0.708 W cm^{-2}. To the best of our knowledge, this is the highest P_{max} reported so far for DHFC with oxygen as the oxidant (Table S1).

3.2. Effects of PBI membrane thickness

Fig. 3a-d compares the OCV, polarization performance and high-frequency resistance (HFR) of DHFC operated with different-thickness of PBI membranes (20, 50, and 100 μm). As the thickness of the PBI membrane increased, the DHFC exhibited higher OCV (Fig. 3a). The increase was caused by the lower N_2H_4 crossover form anode to cathode when a thicker PBI membrane was used. Correspondingly, DHFC with a thicker membrane (50 and 100 μm) exhibited a higher operation voltage than the thinnest membrane (20 μm) at a low current density (<0.2 A cm^{-2}, Fig. 3c, region A) [27]. However, at a larger current density, the

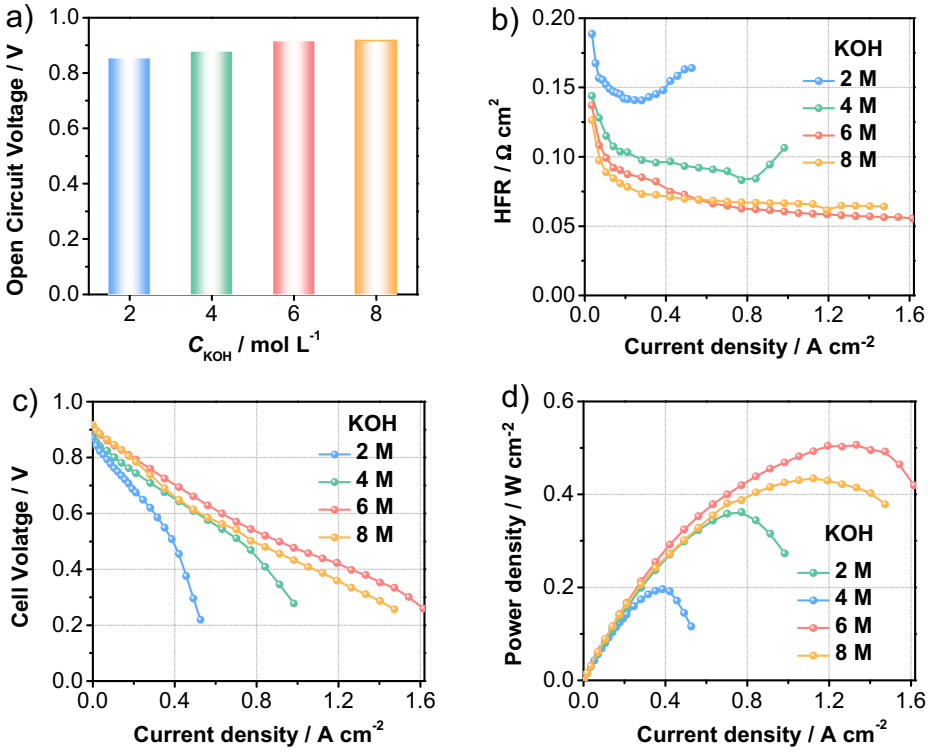

Fig. 1. (a-d) Effects of KOH concentration. (a) Relationship between OCV and KOH concentration in the anolyte. (b) High-frequency resistance (HFR) and (c) polarization and (d) power density curves of DHFC fed with different concentrations of KOH (2 M to 8 M). N_2H_4 concentration was controlled at 0.5 M. Test conditions: Oxygen was used as oxidant with 100% RH. Cell temperature was controlled at 80 °C.

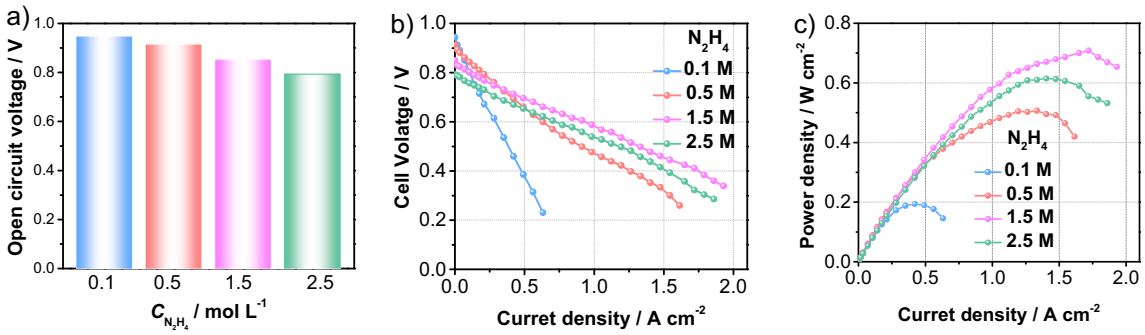

Fig. 2. (a-c) Effects of N_2H_4 concentration. (a) Variation of OCV of DHFC with increasing N_2H_4 concentration in the anolyte. (b) Polarization and (c) power density curves of DHFC fed with different concentrations of N_2H_4 solution (0.1 M to 2.5 M). 6 M KOH was used. Test conditions: Oxygen was used as oxidant with 100% RH. Cell temperature was controlled at 80 °C. Hydrazine hydrate is miscible with water and thus enables the usage of high concentration of N_2H_4 solution (i.e., 2.5 M).

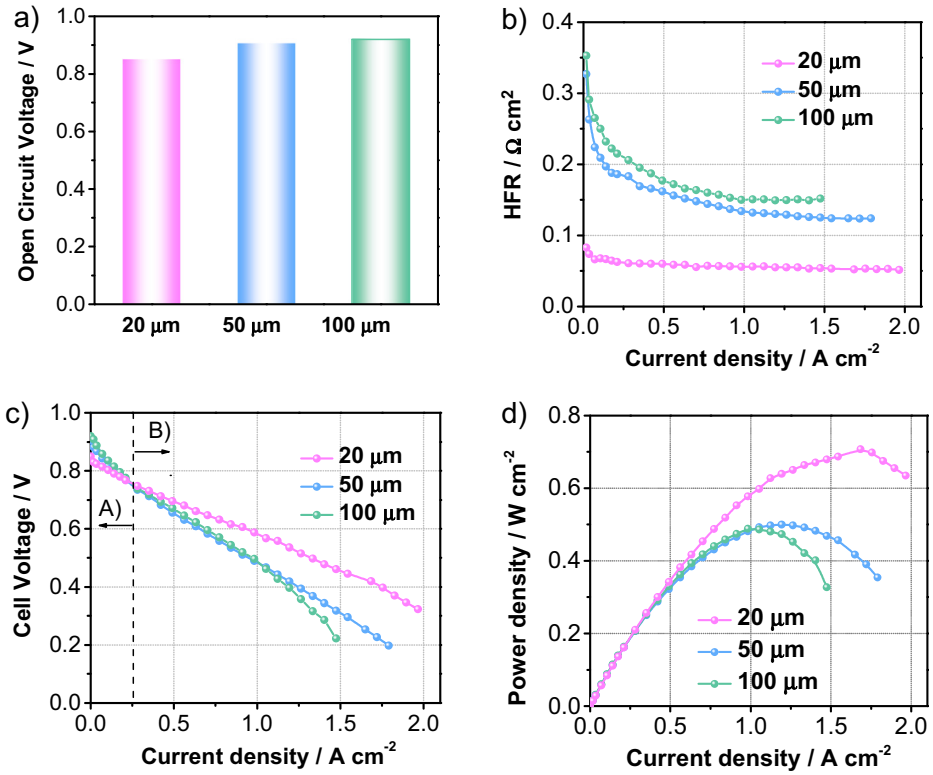

Fig. 3. (a) Relationship between OCV and membrane thickness. (b) high-frequency resistance (HFR) and (c) polarization and (d) power density curves and of DHFC operated with different-thicknesses of KOH-doped PBI membrane (20, 50, and 100 μm). Test conditions: 1.5 M N_2H_4 in 6 M KOH solution was fed as the fuel; oxygen was used as the oxidant with 100% RH. Cell temperature was controlled at 80 °C.

polarization performance of DHFC operated with the 20-μm PBI membrane was superior to that of a thicker membrane (Fig. 3c, region B). The better polarization performance of the 20-μm PBI membrane in a larger current density region (ohmic-resistance-controlled region) is attributed to the low membrane resistance (Fig. 3b) [28]. This result also indicates that the PBI membrane has excellent N_2H_4-resistance properties, which enables the usage of the thinner membrane (e.g., 20 μm) to minimize the ohmic loss and thus maintain higher output power density (Fig. 3d).

3.3. Effects of oxygen humidity

Apart from anolyte and membrane thickness, cathode gas humidity is another parameter that influences the polarization performance of DHFCs operated with KOH-doped PBI membranes. Based on the cathode ORR, H_2O, as a reactant, was consumed in the cathode catalyst layer [29]. Therefore, water content in the cathode catalyst layer is critical for the oxygen reduction reaction and consequently the cell polarization performance. Fig. 4 shows the polarization performance of DHFC under different cathode humidification temperatures. When the cathode humidification temperature increased from 40 °C to 80 °C (100% RH), the polarization performance at the all-current–density range was improved. However, as relative humidity surpasses 100% (e.g., 90 °C), oxygen transport in the cathode catalyst layer at large current density would be impeded because of water flooding [30]. Therefore, at large current density (>0.4 A cm^{-2}), the polarization performance at 90 °C was inferior to that at 80 °C.

3.4. Comparison of the three types of electrolyte membranes

To further evaluate the feasibility of KOH-doped PBI membrane for DHFC, two other commonly used membranes [Na^+-type Nafion membrane and ammonium-type anion exchange membrane

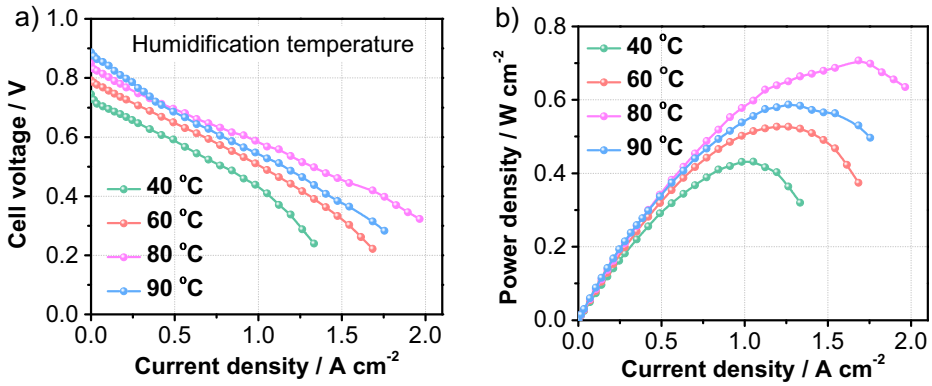

Fig. 4. (a) Polarization and (b) power density curves of DHFC under different cathode humidification temperatures from 40 °C to 90 °C. Test conditions: 1.5 M N_2H_4 in 6 M KOH solution. Oxygen was used as the oxidant. Cell temperature was controlled at 80 °C.

(QAPS)] for DHFC were also tested for comparison. The thickness of the three types of membranes was nearly 20 μm. For liquid-fed fuel cells, membrane permeation is a critical parameter for the cell polarization performance, especially in the low-current-density region [8,31,32]. According to precious studies [33–35], fuel crossover can be measured by linear sweep voltammetry (LSV) method with anode and cathode fed with fuel and humified N_2, respectively. Fuel (e.g., N_2H_4) permeated from the anode is oxidized at the cathode. Therefore, the oxidation current density can be recognized as an indicator to describe the permeation property of membrane. Lower oxidation current gives lower permeability of N_2H_4, which implies better fuel-resistance properties of membranes. As shown in Fig. 5a, the fuel-resistance properties of the KOH-doped PBI membrane (1.3×10^{-7} mole s^{-1} cm^{-2}) was much better than that of the Na^+-type Nafion membrane (7×10^{-7} mole s^{-1} cm^{-2}) but slightly worse than that of the ammonium-type anion exchange membrane (QAPS, 1.1×10^{-7} mole s^{-1} cm^{-2}). Consequently, in the low-current-density region, the polarization performance of DHFC using KOH-doped PBI membrane was close to that using QAPS, both of which are significantly higher than that using the Na^+-type Nafion membrane (Fig. 5c). However, the ion conductivity of the KOH-doped PBI membrane was significantly higher than that of QAPS and Na^+-type Nafion membrane, as evidenced by the fact that membrane resistance of KOH-doped PBI membrane was nearly 0.05 Ω cm^2, which is two and four times lower than that of QAPS (0.1 Ω cm^2) and Na^+-type Nafion membrane (0.2 Ω cm^2), respectively (Fig. 4b). Therefore, at a larger current density (ohmic-resistance-controlled region), the DHFC operated with the KOH-doped PBI membrane exhibited the highest polarization performance with a peak power density of 0.708 W cm^{-2} (Fig. 5d) [28]. Although KOH-doped PBI is promising for DHFC, there are still some challenges remained in the long-term

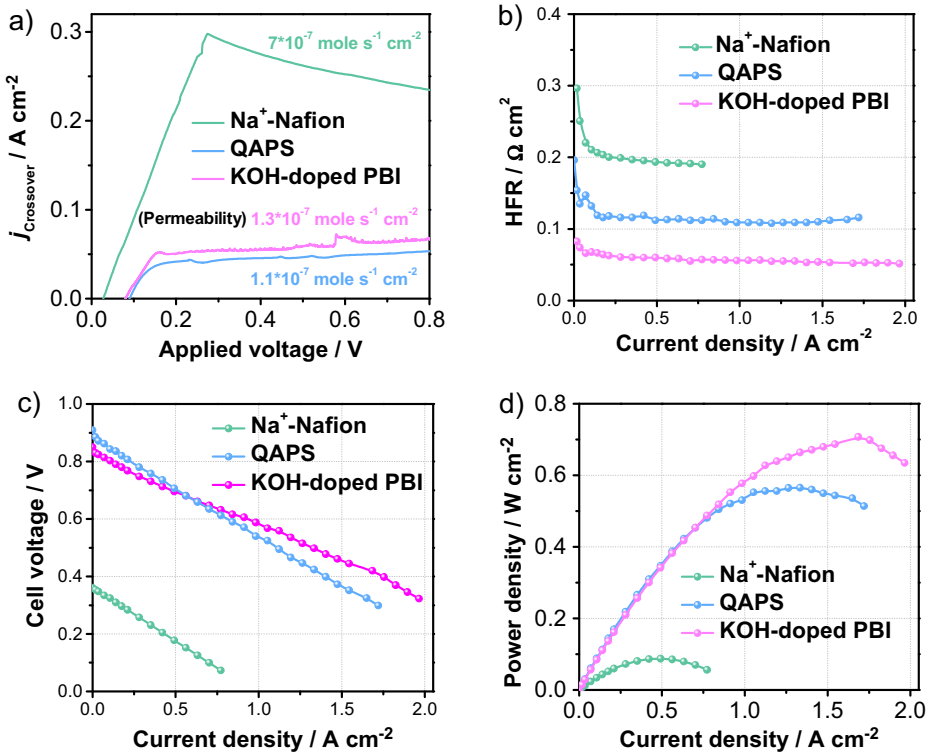

Fig. 5. (a) Crossover current density of DHFC with different types of membranes. (b) High-frequency resistance (HFR) and (c) polarization and (d) power density curves of DHFC operated with different types of membranes. Test conditions: 1.5 M N_2H_4 in 6 M KOH solution. Oxygen was used as the oxidant with 100% RH. Cell temperature was controlled at 80 °C. LSV experiment conditions: Scanning from 0 V to 0.8 V with a scan rate of 2 mV s^{-1}.

durability: (i) Polybenzimidazole is chemically unstable in aqueous KOH, which may affect the long-term durability of PBI membrane-based DHFC [36]. (ii) Recovering dehydrated PBI membrane during fuel cell start-up/shut-down process is still challenging.

4. Conclusion

A KOH-doped PBI membrane was applied in DHFC, and the detailed operating conditions were investigated for the first time. With optimized KOH and N_2H_4 concentrations in the anolyte, membrane thickness, and cathode humification temperature, a peak power density of 0.708 W cm^{-2} was achieved. Compared with the two other commonly used membranes [Na^+-type Nafion membrane and ammonium-type anion ion exchange membrane], the KOH-doped PBI membrane exhibited excellent membrane permeation property and the highest ion conductivity, thus obtaining the highest peak power density and demonstrating its promising application in DHFCs.

Declaration of Competing Interest

The authors declare that they have no known competing financial interests or personal relationships that could have appeared to influence the work reported in this paper.

Acknowledgments

Z.-Y. Z., Y.-C. W., Q. W., L.-Y. W., Y. H. and Y.-H. H., were financially supported by National Key Research and Development Program of China (2017YFA0206500) and L. H was supported by National Science Foundation of China 21805121).

Appendix A. Supplementary material

Supplementary data to this article can be found online at https://doi.org/10.1016/j.jcis.2019.12.046.

References

[1] A. Serov, C. Kwak, Appl. Catal. B Environ. 98 (2010) 1–9.
[2] K. Yamada, K. Yasuda, H. Tanaka, Y. Miyazaki, T. Kobayashi, J. Power Sources 122 (2003) 132–137.
[3] K. Yamada, K. Asazawaa, K. Yasudab, T. Ioroib, H. Tanakaa, Y. Miyazakib, T. Kobayashib, J. Power Sources 115 (2003) 236–242.
[4] S.J. Lao, H.Y. Qin, L.Q. Ye, B.H. Liu, Z.P. Li, J. Power Sources 195 (2010) 4135–4138.
[5] L. Gubler, S.M. Dockheer, W.H. Koppenol, J. Electrochem. Soc. 158 (2011) B755–B769.
[6] D. Banham, S. Ye, K. Pei, J.-I. Ozaki, T. Kishimoto, Y. Imashiro, J. Power Sources 285 (2015) 334–348.
[7] H. Qin, Z. Liu, Y. Guo, Z. Li, Int. J. Hydrogen Energy 35 (2010) 2868–2871.
[8] K. Yamada, K. Yasuda, N. Fujiwara, Z. Siroma, H. Tanaka, Y. Miyazaki, T. Kobayashi, Electrochem. Commun. 5 (2003) 892–896.
[9] J. Jeong, M. Choun, J. Lee, Angew. Chem. Int. Ed. 56 (2017) 13513–13516.
[10] K. Matsuoka, Y. Iriyama, T. Abe, M. Matsuoka, Z. Ogumi, J. Power Sources 150 (2005) 27–31.
[11] K. Asazawa, T. Sakamoto, S. Yamaguchi, K. Yamada, H. Fujikawa, H. Tanaka, K. Oguro, J. Electrochem. Soc. 156 (2009) B509.
[12] F. Zhang, H. Zhang, C. Qu, J. Ren, J. Power Sources 196 (2011) 3099–3103.
[13] F. Zhang, H. Zhang, J. Ren, C. Qu, J. Mater. Chem. 20 (2010) 8139.
[14] G. Liu, H. Zhang, J. Hu, Y. Zhai, D. Xu, Z.-G. Shao, J. Power Sources 162 (2006) 547–552.
[15] P. Moçotéguy, B. Ludwig, J. Scholta, Y. Nedellec, D.J. Jones, J. Rozière, Fuel Cells 10 (2010) 299–311.
[16] A. Chandan, M. Hattenberger, A. El-kharouf, S. Du, A. Dhir, V. Self, B.G. Pollet, A. Ingram, W. Bujalski, J. Power Sources 231 (2013) 264–278.
[17] L.-Y. Li, B.-C. Yu, C.-M. Shih, S.J. Lue, J. Power Sources 287 (2015) 386–395.
[18] B. Sana, A. Das, T. Jana, Polymer 172 (2019) 213–220.
[19] W.-T. Chang, Y.-H. Chao, C.-W. Li, K.-L. Lin, J.-J. Wang, S.R. Kumar, S.J. Lue, J. Power Sources 414 (2019) 86–95.
[20] B. Xing, O. Savadogo, Electrochem. Commun. 2 (2000) 697–702.
[21] T. Wang, Q. Wang, Y. Wang, Y. Da, W. Zhou, Y. Shao, D. Li, S. Zhan, J. Yuan, H. Wang, Angew. Chem. Int. Ed. 131 (2019) 2–8.
[22] J. Pan, C. Chen, Y. Li, L. Wang, L. Tan, G. Li, X. Tang, L. Xiao, J. Lu, L. Zhuang, Energy Environ. Sci. 7 (2014) 354–360.
[23] D. Aili, M.K. Hansen, R.F. Renzaho, Q.F. Li, E. Christensen, J.O. Jensen, N.J. Bjerrum, J. Memb. Sci. 447 (2013) 424–432.
[24] W.X. Yin, Z.P. Li, J.K. Zhu, H.Y. Qin, J. Power Sources 182 (2008) 520–523.
[25] M.R. Kraglund, D. Aili, K. Jankova, E. Christensen, Q. Li, J.O. Jensen, J. Electrochem. Soc. 163 (2016) F3125–F3131.
[26] H.Y. Qin, Z.X. Liu, W.X. Yin, J.K. Zhu, Z.P. Li, J. Power Sources 185 (2008) 895–898.
[27] J.G. Liu, T.S. Zhao, Z.X. Liang, R. Chen, J. Power Sources 153 (2006) 61–67.
[28] P. Argyropoulos, K. Scott, A.K. Shukla, C. Jackson, J. Power Sources 123 (2003) 190–199.
[29] Y. Chang, Y. Qin, Y. Yin, J. Zhang, X. Li, Appl. Energy 230 (2018) 643–662.
[30] T.J. Omasta, A.M. Park, J.M. LaManna, Y. Zhang, X. Peng, L. Wang, D.L. Jacobson, J.R. Varcoe, D.S. Hussey, B.S. Pivovar, W.E. Mustain, Energy Environ. Sci. 11 (2018) 551–558.
[31] R.Z. Jiang, D.R. Chu, J. Electrochem. Soc. 151 (2004) A69–A76.
[32] W. Xu, T. Lu, C. Liu, W. Xing, Electrochim. Acta 50 (2005) 3280–3285.
[33] K. Ramya, K.S. Dhathathreyan, J. Electroanal. Chem. 542 (2003) 109–115.
[34] Y.-W. Rhee, S.Y. Ha, R.I. Masel, J. Power Sources 117 (2003) 35–38.
[35] J.J. Giner-Sanz, E.M. Ortega, V. Pérez-Herranz, Int. J. Hydrogen Energy 39 (2014) 13206–13216.
[36] D. Aili, K. Jankova, Q.F. Li, N.J. Bjerrum, J.O. Jensen, J. Memb. Sci. 492 (2015) 422–429.